

Low-speed limit of Bohr's stopping-power formula

Peter Sigmund

Physics Department, Odense University, DK-5230 Odense M, Denmark

(Received 18 March 1996)

Bohr's classical (nonrelativistic) model of charged-particle stopping is evaluated explicitly for arbitrary values of projectile charge and speed. This removes the logarithmic cutoff from the original expression and generates a stopping formula which can be utilized also to extend the range of practical applicability of Bloch's theory. As expected such a formulation appears to be a better starting point than the Born approximation for estimating stopping powers of heavy ions at velocities $v < Z_1 e^2 / \hbar$. [S1050-2947(96)07508-7]

PACS number(s): 34.50.Bw; 61.85.+p; 52.40.Mj; 79.20.Rf

I. INTRODUCTION

In a classic paper "On the Theory of the Decrease of Velocity of Moving Electrified Particles on Passing Through Matter," Bohr [1] derived an expression for the stopping cross section per target electron (charge $-e$, mass m) of a material,

$$S = \frac{4\pi Z_1^2 e^4}{mv^2} \ln \frac{Cmv^3}{Z_1 e^2 \omega}, \quad C = 1.1229 \quad (1)$$

for a swift ion (point-charge $Z_1 e$) in uniform motion (speed v) interacting with a harmonically bound classical electron (resonance frequency ω). Bethe's quantum theory of charged-particle stopping [2] resulted in a formally very similar expression where the main difference was the replacement of the logarithm by $\ln(2mv^2/I)$. Here I is the mean excitation energy which reduces to $\hbar\omega$ in case of one dominating resonance.

Bloch's extension of Bethe's theory [3] contains the two results as limiting cases. Bloch's formula reduces to Bethe's for projectiles of low charge, especially protons and deuterons, while Bohr's result is approached in the limit of

$$\kappa = \frac{2Z_1 v_0}{v} \gg 1, \quad (2)$$

$v_0 = e^2/\hbar$ being the Bohr velocity. A recent rederivation [4] has confirmed and extended the theoretical basis of the Bloch formula.

It was noted long ago [5] that for projectiles of sufficiently high charge at not too high speed, Bohr's formula must be a better starting point for theoretical predictions of stopping powers than Bethe's. Despite this, it is Bethe's theory that has served universally as a basis for computations and compilations of stopping powers, regardless of the magnitude of the projectile charge [6-9]. Although this may seem peculiar at first sight there is at least one plausible reason for the neglect of Bohr's formula: Eq. (1) makes sense only as long as the logarithm is positive, i.e., for

$$\frac{2mv^2}{\hbar\omega} > \frac{\kappa}{C}, \quad (3)$$

while the Bethe logarithm remains positive for $2mv^2/I > 1$. Since $\kappa > 1$ in the range of validity of Bohr's theory, Eq. (1) is inapplicable as it stands over a significantly wider velocity range than the uncorrected Bethe formula. It is, in fact, inapplicable in the regime where on physical grounds it would be a most useful replacement for the Bethe formula.

This limitation of Bohr's formula originates in the application of an asymptotic expansion which could easily have been avoided if the need had been obvious at the time: Eq. (1) was originally derived for swift α particles where Eq. (3) was no serious limitation. The present paper serves the purpose to eliminate this handicap and thus to present a formulation of Bohr's theory which reflects its physical input. The limitations of the physical model will be mentioned briefly.

The Bloch formula [3] shows likewise a rather high lower cutoff velocity because of the use of an asymptotic expansion. The present treatment can be utilized to modify also the low-speed limit of the Bloch formula at least for large values of κ .

II. BOHR'S THEORY

Bohr's theory considers close and distant interactions separately. Close collisions are treated as free-Coulomb interactions, resulting in the following dependence of the energy transfer T versus impact parameter p :

$$T_{\text{close}} = \frac{2Z_1^2 e^4}{mv^2 p^2} \frac{1}{1 + (b/2p)^2}, \quad (4)$$

where $b = 2Z_1 e^2 / mv^2$ is the collision diameter. (This relation follows directly from Rutherford's law $\tan(\theta/2) = b/2p$ and $T = 2mv^2 \sin^2 \theta/2$, θ denoting the center-of-mass scattering angle.)

Binding of target electrons is taken into account in distant interactions and enters through a classical resonance frequency ω ; the electric field of the projectile is taken in the dipole limit, i.e., its spatial variation across the diameter of the atom is ignored. This yields

$$T_{\text{dist}} = \frac{2Z_1^2 e^4}{mv^2 p^2} \left\{ \left[\frac{\omega p}{v} K_0 \left(\frac{\omega p}{v} \right) \right]^2 + \left[\frac{\omega p}{v} K_1 \left(\frac{\omega p}{v} \right) \right]^2 \right\}, \quad (5)$$

where K_0 and K_1 are modified Bessel functions in standard notation [10]. The stopping cross section is then given by

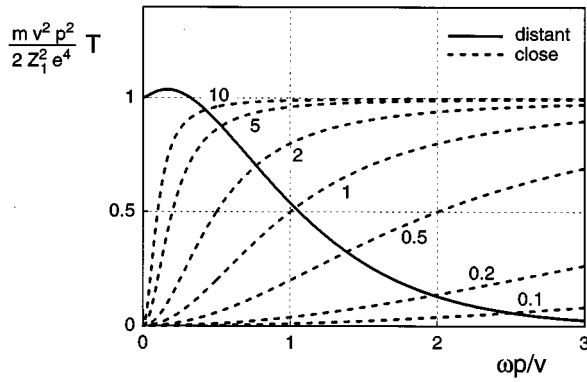


FIG. 1. Energy-loss functions T_{dist} and T_{close} vs impact parameter p . In the chosen units T_{dist} is a universal curve, while T_{close} depends on projectile speed through the Bohr parameter $\xi = mv^3/Z_1 e^2 \omega$. Curves refer to values of $0.1 < \xi < 10$. The crossover is taken as the limiting impact parameter p_0 which likewise depends on ξ (Fig. 2).

$$S = S_{\text{close}} + S_{\text{dist}} = \int_0^{p_0} 2\pi p dp T_{\text{close}}(p) + \int_{p_0}^{\infty} 2\pi p dp T_{\text{dist}}(p), \quad (6)$$

where p_0 is a critical impact parameter separating close from distant interactions.

The two integrations can be carried out and lead to

$$S_{\text{close}} = \frac{2\pi Z_1^2 e^4}{mv^2} \ln \left[1 + \left(\frac{2p_0}{b} \right)^2 \right] \quad (7)$$

and

$$S_{\text{dist}} = \frac{4\pi Z_1^2 e^4}{mv^2} \frac{\omega p_0}{v} K_0 \left(\frac{\omega p_0}{v} \right) K_1 \left(\frac{\omega p_0}{v} \right). \quad (8)$$

Bohr's evaluation is based on the recognition that, at high speed where $b \ll v/\omega$, a value of p_0 may be found such that $b \ll p_0 \ll v/\omega$. If so, the Bessel functions may be represented by their expansions for small arguments,

$$\zeta K_0(\zeta) K_1(\zeta) \sim \ln(2/\zeta) - \gamma + O(\zeta^2), \quad (9)$$

where $\gamma = 0.5772$ is Euler's constant, and Eqs. (7) and (8) simplify to

$$S_{\text{dist}} \approx \frac{4\pi Z_1^2 e^4}{mv^2} \ln \frac{2ve^{-\gamma}}{\omega p_0}, \quad S_{\text{close}} \approx \frac{4\pi Z_1^2 e^4}{mv^2} \ln \frac{2p_0}{b}. \quad (10)$$

Summation leads to Eq. (1) with $C = 2 \exp(-\gamma)$.

Note that the limiting impact parameter p_0 drops out since within the same approximation, $T_{\text{close}}(p_0) = T_{\text{dist}}(p_0) \approx 2Z_1^2 e^4 / mv^2 p_0^2$ for $b \ll p_0 \ll v/\omega$.

III. STRAIGHT EVALUATION

Figure 1 shows T_{dist} and T_{close} versus impact parameter p for several projectile speeds, expressed by the Bohr parameter $\xi = mv^3/Z_1 e^2 \omega$ ranging from the high-speed regime ($\xi = 10$) down to $\xi = 0.1$, i.e., an order of magnitude below the threshold expressed by Eq. (3). It is evident that there is

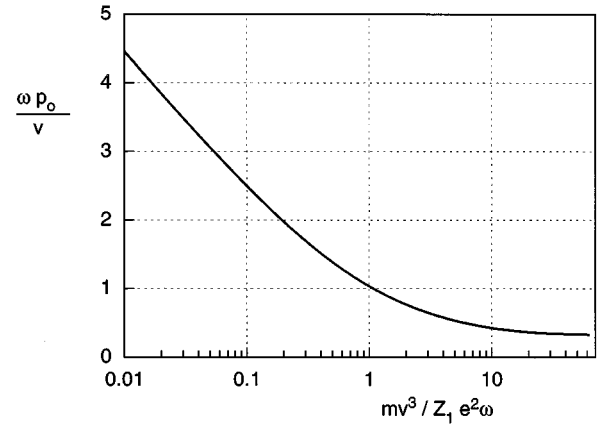


FIG. 2. Variation with projectile speed (expressed by Bohr parameter $\xi = mv^3/Z_1 e^2 \omega$) of the limiting impact parameter p_0 (expressed in multiples of the adiabatic radius v/ω) separating close from distant collisions.

always a crossover point p_0 where $T_{\text{close}}(p_0) = T_{\text{dist}}(p_0)$ and that S must be positive for all values of ξ . Figure 2 shows this crossover as a function of ξ , determined algebraically from the inverse relation $\xi = \xi(\omega p_0/v)$. This relation, together with $S = S(\omega p_0/v)$ [Eqs. (7) and (8)], defines a parameter representation of the dependence of the stopping cross-section (6) on the Bohr parameter ξ . The result may be expressed in a universal form via the stopping number L defined by

$$S = \frac{4\pi Z_1^2 e^4}{mv^2} L \left(\frac{mv^3}{Z_1 e^2 \omega} \right). \quad (11)$$

L is shown in Fig. 3 together with Bohr's asymptotic expression (1). The two curves are parallel and almost coincident at high projectile speed but differ significantly for $\xi < 3$. For qualitative orientation the contributions from close and dis-

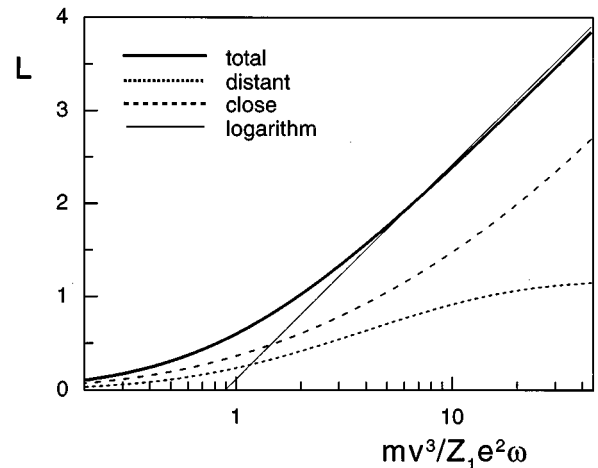


FIG. 3. Stopping number L vs Bohr parameter $\xi = mv^3/Z_1 e^2 \omega$. Thick solid line: Straight evaluation of Eq. (6); contributions from close and distant collisions included separately [Eqs. (7) and (8)]; thin line: Bohr formula Eq. (1).

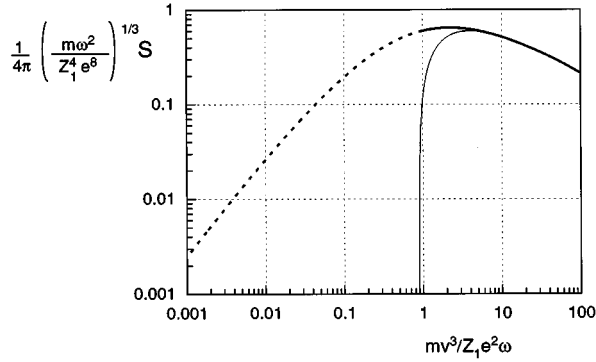


FIG. 4. Stopping cross-section S [expressed by $L(\xi)/\xi^{2/3}$] vs Bohr parameter $\xi = mv^3/Z_1 e^2 \omega$ found by replotting data from Fig. 3. The stipled part ($\xi < 1$) of the curve reflects the need for various corrections to the Bohr theory (see text in Sec. IV).

tant interactions have also been included separately. It is seen that close interactions dominate at all projectile speeds, in particular so at low values of ξ where p_0 increases monotonically according to Fig. 2.

Surprisingly, the high-speed behavior does not reflect the commonly accepted equipartition between close and distant contributions to the stopping cross section. This feature is related to the overshoot of the distant contribution at small values of $\omega p/v$ in Fig. 1 which results in a nonvanishing asymptotic value of p_0 at high ξ as seen in Fig. 2. It is most likely an artifact which also causes the minute difference between the two curves in Fig. 3 at high ξ and which could be avoided by a smoother interpolation procedure. The point is not followed up here since Fig. 1 indicates that the detailed interpolation procedure is not crucial in the determination of the total stopping cross section.

Figure 4 shows the function $L(\xi)/\xi^{2/3}$ which represents a universal plot of the stopping cross section itself. Also included is Bohr's expression Eq. (1). The double-logarithmic plot emphasizes close agreement at high speed and drastically different behavior at low speed. The powerlike behavior at low speed can be approximated by the relation

$$\frac{L}{\xi^{2/3}} \sim 5.45 \xi^{1.114} \quad \text{for } \xi < 0.01 \quad (12)$$

which is equivalent with a stopping cross section $\propto v^{3.3}$.

IV. DISCUSSION

Bohr's original evaluation was geared toward large values of the Bohr parameter $\xi = mv^3/Z_1 e^2 \omega$, for which there is a range of impact parameters where the assumptions of free-Coulomb scattering (close collisions) and dipole approximation for the electric field (distant collisions) are fulfilled simultaneously. In that limit the value chosen for the critical impact parameter p_0 is immaterial as long as it falls within the bounds given above. Figure 1 shows that this picture is valid approximately for $\xi \geq 10$, depending on the desired accuracy. For $\xi < 10$ the value of p_0 matters, but if p_0 is defined as the crossover, the physical picture should remain basically correct.

Figure 5 shows a comparison of literature values of stop-

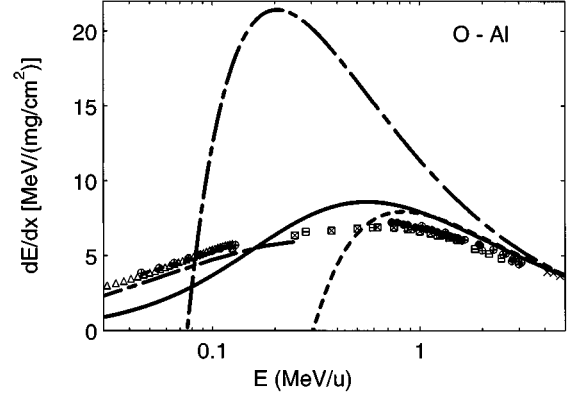


FIG. 5. Stopping power of aluminium estimated for bare oxygen ion with $I = \hbar \omega = 166$ eV [11]. Solid line: Present result; dotted line: Bohr formula Eq. (1); dot-dashed line: Bethe formula without shell correction; experimental data for equilibrium charge states compiled in [12].

ping powers for oxygen in aluminium [12] with the uncorrected Bethe formula, the uncorrected Bohr formula and the modified Bohr formula. It is seen that the mere removal of the cutoff generates a stopping formula which predicts the trend of the experimental data. No correction has been applied to account for the screening of the projectile charge. Figure 5 indicates that at least for this system, an effective-charge correction necessary to fit experimental data would have to be much smaller than in the familiar situation where the Bethe formula has been used as a theoretical basis. An effective-charge correction is significant mainly for distant collisions. According to Fig. 3, the contribution from distant interactions is less than that from close interactions. Therefore, starting at Bohr's formulation deaccentuates the need for an effective-charge correction. This is an important physical distinction but also a significant simplification from the point of view of tabulating stopping powers.

The use of a single resonance frequency is an oversimplification, in particular, at the low-velocity end in Fig. 5 where the theoretical curve drops below the experimental points. This restriction needs to be removed in a detailed comparison with experimental data [13].

Despite the apparent success of the description—considering the lack of a charge-state correction—several obvious limitations need to be mentioned. Most of all, the validity of the dipole approximation is limited to large impact parameters. Now, this approximation is applied for $p > p_0$, and since p_0 increases with decreasing ξ (Fig. 2) the error might be tolerable. For a rough estimate we may consider the ratio p_0/a , where $a \approx a_0 Z_2^{-1/3}$ is the Thomas-Fermi radius of a target atom. With $\hbar \omega \approx Z_2 e^2 / 2a_0$ one finds

$$\frac{p_0}{a} \sim \left(\frac{4Z_1}{Z_2} \xi \right)^{1/3} \frac{\omega p_0}{v}, \quad (13)$$

where the dependence of $\omega p_0/v$ on ξ is given by Fig. 2. Here the factor $\xi^{1/3} \omega p_0/v$ equals 1 at $\xi = 1$ and varies very slowly for $\xi < 1$. It is thus the factor $(4Z_1/Z_2)^{1/3}$ that determines the quality of the dipole approximation.

Quantitatively, deviations from the dipole approximation enter via target polarization in Bohr's theory [14]. The per-

inent parameter is the Barkas parameter $Z_1 e^2 \omega / m v^3 = 1/\xi$ [15]. This suggests that discrepancies can be expected when the modified Bohr formula is applied in the range of $\xi < 1$. Note, however, that a polarization-corrected Bohr model of stopping still predicts a universal scaling relation $L = L(\xi)$ in the absence of a charge-state correction.

The low-velocity cutoff in the Bethe formula shown in Fig. 5 is related to the neglect of shell corrections, i.e., the neglect of the internal motion of target electrons. Such corrections, which also cause a decrease of the stopping-power maximum, must be presumed also to enter the Bohr theory, although a detailed study is missing. Within the range of validity of the classical-oscillator model they drop out in the dipole limit, but according to kinetic theory [16] close collisions provide a contribution similar to the one entering the Bethe theory. This would predict a correction of the relative magnitude $\sim -\overline{v_e^2}/v^2$, where $\overline{v_e^2}$ is the mean-square velocity of the target electron. For a Thomas-Fermi atom with atomic number Z_2 and $\overline{v_e^2} \sim Z_2^{4/3} v_0$ and $\hbar \omega \sim Z_2 e^2 / 2a_0$ this would suggest a ratio

$$\frac{(\text{shell correction})}{(\text{Barkas factor})} \sim \frac{-\overline{v_e^2}/v^2}{1/\xi} \sim -\frac{4Z_2^{1/3}}{\kappa}, \quad (14)$$

indicating comparable magnitudes of the two corrections but dependent in detail on atomic numbers of projectile and target.

V. MODIFIED BLOCH FORMULA

According to Bloch [3], the stopping cross section of an atom is determined by the following expression for the stopping number,

$$L = \sum_n f_{0n} \left[\ln \frac{2mv^2}{\hbar \omega_{n0}} + \psi(1) - \text{Re} \psi \left(1 + i \frac{Z_1 e^2}{\hbar v} \right) \right], \quad (15)$$

where $\psi(x) = d \ln \Gamma(x) / dx$ and Re denotes the real part. The quantities ω_{n0} and f_{0n} represent the transition frequencies and associated dipole-oscillator strengths of a target atom (or molecule) for the n th excitation level above ground state with

$$\sum_n f_{0n} = 1 \quad \text{and} \quad \ln I = \sum_n f_{0n} \ln(\hbar \omega_{n0}), \quad (16)$$

where I is the mean excitation energy. The first term within the brackets of Eq. (15) represents Bethe's result excluding shell and relativistic corrections as well as polarization and density effects. The second and third term taken together represent the Bloch correction which does not contain target parameters.

Equation (15) may be rearranged in the form

$$L = \sum_n f_{0n} \left[\ln \frac{C m v^3}{Z_1 e^2 \omega_{n0}} + \ln \frac{Z_1 e^2}{\hbar v} - \text{Re} \psi \left(1 + i \frac{Z_1 e^2}{\hbar v} \right) \right]. \quad (17)$$

Here the first term represents the stopping due to an ensemble of classical Bohr oscillators with resonance frequencies ω_{n0} . The second and third term taken together do not contain target parameters and depend only on Bohr's κ pa-

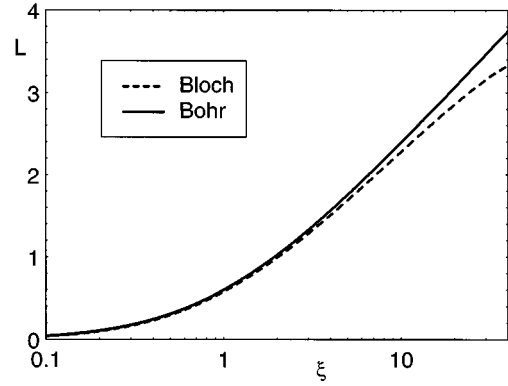


FIG. 6. Stopping number from modified Bloch formula compared to the result from the modified Bohr formula, labeled “total” in Fig. 3. The parameter $\alpha = (Z_1^2 e^2 / a_0 \hbar \omega)^{1/3}$ has been set equal to 2.

rameter defined in Eq. (2). In the classical limit expressed by Eq. (2), this term goes as [10]

$$\ln \frac{Z_1 e^2}{\hbar v} - \text{Re} \psi \left(1 + i \frac{Z_1 e^2}{\hbar v} \right) \sim -\frac{1}{3\kappa^2} - \frac{2}{15\kappa^4} \dots \quad (18)$$

It appears tempting to replace the Bohr logarithm in the first term in Eq. (17) by the function derived in Sec. III and in this way to generate a modified Bloch formula which does not turn negative at low projectile speed. This is illustrated for the case of one dominating transition frequency ω in Fig. 6, where κ has been replaced by

$$\kappa = \frac{2\alpha}{\xi^{1/3}} \quad \text{with} \quad \alpha = Z_1^{2/3} \left(\frac{e^2 / a_0}{\hbar \omega} \right)^{1/3}. \quad (19)$$

Figure 6 shows that for $\alpha = 2$, the stopping number according to the modified Bloch formula approaches that of the modified Bohr formula at low speed while a difference occurs at high speed which, in essence, is the difference between the straight Bethe and the unmodified Bohr formula. This difference increases with decreasing α —i.e., when the Bloch formula approaches the Bethe limit—while it diminishes rapidly for larger values of α . Already for $\alpha = 4$ the difference becomes invisible on the scale of Fig. 6.

In the opposite limit, for small values of κ , the Bloch formula approaches Bethe's result. This corresponds to large values of ξ in Fig. 1, where the difference between the modified and the unmodified Bohr formula becomes negligible. Hence, the present modification does not noticeably affect the Bethe limit of the Bloch formula.

ACKNOWLEDGMENTS

Thanks are due to H. Paul for providing access to his files of stopping data and to H. H. Mikkelsen for useful comments. This work has been supported by the Danish Natural Science Research Council (SNF).

- [1] N. Bohr, *Philos. Mag.* **25**, 10 (1913).
- [2] H. Bethe, *Ann. Phys. (Leipzig)* **5**, 324 (1930).
- [3] F. Bloch, *Ann. Phys. (Leipzig)* **16**, 285 (1933).
- [4] J. Lindhard and A. H. Sørensen, *Phys. Rev. A* **53**, 2443 (1996).
- [5] U. Fano, *Annu. Rev. Nucl. Sci.* **13**, 1 (1963).
- [6] L. C. Northcliffe and R. F. Schilling, *Nucl. Data Tables A* **7**, 233 (1970).
- [7] F. Hubert, A. Fleury, R. Bimbot, and D. Gardes, *Ann. Phys. (Paris)* **5 S**, 1 (1980).
- [8] J. F. Ziegler, *Handbook of Stopping Cross Sections for Energetic Ions in All Elements* (Pergamon, New York, 1980), Vol. 5.
- [9] F. Hubert, R. Bimbot, and H. Gauvin, *At. Data Nucl. Data Tables* **46**, 1 (1990).
- [10] *Handbook of Mathematical Functions* edited by M. Abramowitz and I. A. Stegun (Dover, New York, 1964).
- [11] ICRU, *Stopping Powers and Ranges for Protons and Alpha Particles* (ICRU, International Commission of Radiation Units and Measurements, 1994), Vol. 49.
- [12] H. Paul and M. J. Berger, *Atomic and Molecular Data Needed in Radiotherapy* (IAEA-TECDOC-799, Vienna, 1995), p. 415; also personal communication with H. Paul.
- [13] H. H. Mikkelsen, P. Sigmund, and H. Paul (unpublished).
- [14] J. C. Ashley, R. H. Ritchie, and W. Brandt, *Phys. Rev. B* **5**, 2393 (1992).
- [15] J. Lindhard, *Nucl. Instrum. Methods* **132**, 1 (1976).
- [16] P. Sigmund, *Phys. Rev. A* **26**, 2497 (1982).